Articles

Polydimethylsiloxane Networks at Equilibrium Swelling: Extracted and Nonextracted Networks

António N. Falcão,*,† Jan Skov Pedersen, and Kell Mortensen

Department of Solid State Physics, Risø National Laboratory, DK-4000 Roskilde, Denmark

François Boué

Laboratoire Léon-Brillouin, Laboratoire mixte CEA−CNRS, Saclay, France

Received May 26, 1994; Revised Manuscript Received October 3, 1994[⊗]

ABSTRACT: The influence of the extractable components in the microscopic structure of swollen polymer networks was assessed by measuring the small-angle neutron scattering function of extracted and nonextracted networks. The study was done as a function of cross-link density. The scattering data are analyzed using a model cross section that introduces two characteristic length scales: ξ_S, distance below which single chain behavior is dominant, and ξ_L, distance above which large-scale fluctuations of polymer concentration are no longer observed. The correlation length ξ_L and the intensity scattered in the limit of zero scattering vector obtained from the scattering data, for both the extracted and nonextracted systems, scale with polymer concentration with a power law of $(-^3/_2)$. Furthermore, in a double logarithmic plot versus concentration, the experimental points obtained from the extracted and nonextracted systems for ξ_L and $I(q \rightarrow 0)$ fall on the same line within experimental accuracy, suggesting that, in the nonextracted swollen system, the extractable components conform essentially as network strands. The results are compared to predictions of theories based on the percolation model, and with another model that describes the fluctuations in polymer concentration in the swollen system as resulting, for distances below ξ_L, from excluded volume interactions established between large, connected, "hairy-like" units, that result from the attachment of pendant chains and clusters.

1. Introduction

In the last years a large number of small-angle neutron scattering (SANS) studies on cross-linked systems have been performed. Different systems were studied, and the experiments have been done both in the presence of solvent and in the dry state. The experiments were aimed at determining the network structure and the conformation changes that take place upon deformation. Isotropic (e.g. swelling) and nonisotropic (stretching) deformation have been studied, the labeled species being the solvent and/or parts of the network. Upon swelling or stretching, the scattering patterns obtained from the networks exhibit the common feature of the presence of an excess of scattering in the low scattering vector region. This excess scattering is related to the connectivity in the network, and it is observed because the connectivity is revelaed by the presence of the solvent (swelling) or the external action (stretching). Several models have been proposed to explain the processes involved.[1−7] Experiments in which single free chains were incorporated in the networks were recently[8−10] performed. The single chains were either already present in the preparation bath or added, in the presence of solvent, after network preparation. The scattering patterns obtained from these systems also exhibit an excess scattering in the low scattering vector region[8] and this must again result from the revelation of the network connectivity induced, in this case, by the presence of the free chains. When the cross-linking density is low, the mixing of the free chains with the network was found to be random. With increasing cross-link density additional fluctuations appeared, this being interpreted as the result of a progressive approach to complete phase separation between the network and the free chains.[9,10] Within experimental accuracy, the effect was independent of the molecular weight of the free chains. It was suggested that the chains that are present in the state of preparation are expelled from some high cross-linked regions of the network into low cross-linked regions.

Similar effects could be observed in randomly cross-linked networks from which the material not incorporated in the macroscopic cluster is not washed out. This is addressed in the present paper for networks prepared by electron irradiation.

By irradiating a melt of linear polymer chains with high energy, electrons radicals are randomly created. Following diffusion of the chains, the radicals react forming chemical links. At a certain radiation dose threshold, the *gelling dose*, a macroscopic network is formed. With increasing the dose beyond the gelling dose, the weight fraction of the irradiated polymer that will be part of the network first increases exponentially and then saturates, reaching a limit that will be close to unity if the irradiation process has low probability of inducing main-chain scission in the polymer chains. After irradiation, the material not incorporated in the macroscopic network can be removed by standard chemical procedures. The removed material includes

† On leave from Laboratório Nacional de Engenharia e Tecnologia Industrial, P 2685 Sacavém, Portugal.

[⊗] Abstract published in *Advance ACS Abstracts,* November 15, 1994.

0024-9297/96/2229-0809$12.00/0

single polymer chains, but also clusters of several polymer chains. In the following the system free of these removable components will be called *extracted* whereas the irradiated system will be called *nonextracted*.

In a previous paper,[11] structural studies of nonextracted swollen irradiated *polydimethylsiloxane* (PDMS) systems were reported. The studies were done as a function of cross-link density. They included results obtained from macroscopic swelling measurements, from a statistical approach to the cross-linking process, and from scattering experiments in which the intensity scattered by the swollen systems was compared with the intensity scattered by polymer solutions with the same polymer concentration. The scattering data were analyzed by means of a model cross-section that describes the structure as resulting, at large scales, from a fractal arrangement of *particles*, formed by polymer segments (portions of polymer chains), whose average size was identified with the correlation length that characterizes the polymer solution with the concentration present in the swollen network. That correlation length, ξ, is usually associated with the distance below which single chain behavior is observed, i.e., the monomers arrange in a fractal self-avoiding walk characterized by a fractal dimension $D \simeq {}^5/_3$. The model used in the previous paper, introduced two characteristic lengths: ξ_S identified with ξ, and ξ_L, associated with the spatial extent of the fractal fluctuations at large scales, i.e., for $1/\xi_L < q < 1/\xi_S$. In this range, a fractal dimension close to $D_L = {}^5/_3$ was also found, independently of the cross-linking density of the samples. Both ξ_L and the intensity in the limit of zero scattering vector were found to scale with polymer concentration, c_p, as $\xi_L \sim I(q \rightarrow 0) \sim c_p^{-3/2}$.

In the present paper, the influence of the extractable components on the microscopic structure of the swollen system is addressed. The study was done using the small-angle neutron scattering technique, and systems cross-linked to a wide range of cross-linking degrees were measured. The scattering data were analyzed using the model mentioned above. The characterization of the precursor polymer, the sample preparation procedure, and the results of the previous work are first summarized. The results of the small-angle neutron scattering experiments performed in extracted networks are then presented and discussed using as a reference the information previously obtained from nonextracted systems.

2. Experimental Section

2.1. Sample Preparation. The precursor polymer used is a commercially available polydimethylsiloxane (PDMS) with trimethyl termination (the PS047 from Hüls-Petrach). The molecular weight distribution in the polymer melt was characterized[9] by means of gel permeation chromatography (GPC), light scattering, and small-angle neutron scattering. It is a broad distribution with evidence of a long low molecular weight tail that includes a peak in the low limit (see Figure 1). The number average molecular weight, M_n, and the weight average molecular weight, M_w, are respectively $M_n \simeq 16\,000$ and $M_w \simeq 77\,500$, giving the relatively large polydispersity $M_w/M_n \simeq 4.5$.

The samples were produced by irradiating the melt with high-energy electrons, a process that proved to be very reproducible. For the irradiation, the polymer melt was deposited inside cylindrically shaped polyethylene containers. The melt was first centrifuged and then allowed to rest until uniform films were obtained. The typical thickness of the films used in the experiment was around 0.5 mm. Before being irradiated, they were kept, for at least 12 h, under a continuously renewing N_2 atmosphere, in order to remove the oxygen. The samples were then exposed to the 10 MeV electron beam available at the 10 MeV electron accelerator facility of the Risø National Laboratory. Since the presence of oxygen enhances the occurrence of main-chain scission, the samples were kept under N_2 atmosphere during irradiation. This was done by placing the boxes inside plastic bags that were filled with N_2 and sealed.

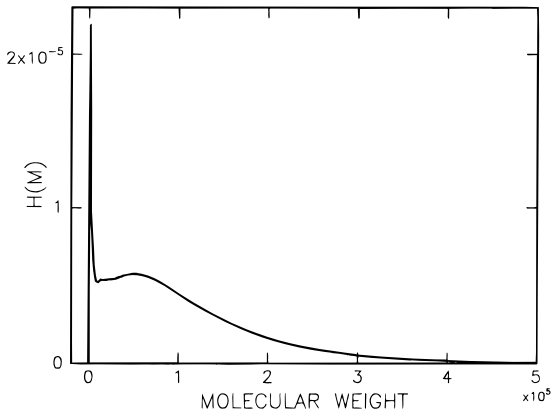

Figure 1. Molecular weight distribution in the precursor polydimethylsiloxane melt.

The total dose received by each sample was deposited in steps. The steps used changed slightly from sample to sample, but were typically around 10 kGy each.

The extraction of the material not incorporated in the macroscopic network was done by immersion of the irradiated systems in a large excess of solvent (more than 100 times the volume of the samples). The solvent (cyclohexane) was renewed every 2 days in the first 2 weeks, and once a week thereafter. The samples were kept in the washing bath for more than 2 months. After being dried, the gel weight fractions were calculated for two of the samples, and the results obtained agreed perfectly with previous results,[11] confirming that the sample preparation process is very reproducible. For the remaining samples, the gel weight fractions were taken from a gel−dose curve that had been determined using many samples coming from several different batches.

Prior to the measurements, the samples were placed inside quartz cuvettes and immersed in an excess of good solvent (fully deuterated *p*-xylene). They were then allowed to rest for a few hours in order to reach the equilibrium swelling degree. It must be recalled that when immersed in a solvent that is good for the polymer, the samples immediately increase volume. The high cross-linked samples rapidly attain their equilibrium swelling volume, V_{eq}, while the lower cross-linked ones reach it a bit more slowly. It was always observed that after a few hours in the presence of the solvent, the volume of the swollen systems changes very little (it is hardly detectable for the networks prepared by irradiation doses higher than 150 kGy) although the complete removal of the extractable components needs a much longer immersion. This suggests that, in the process of solvent absorption, the network expansion is not significantly influenced by the presence of the soluble components. After the equilibrium volume is reached and the soluble part extracted, the volume originally occupied by the latter is essentially replaced by solvent. As a consequence, the polymer volume fraction in the swollen network is roughly

$$c_p^e \simeq \omega_g \times c_p^{ne} \tag{1}$$

where c_p^e and c_p^{ne} represent the polymer volume fraction present in the swollen extracted and nonextracted network, respectively, and w_g the gel weight fraction.

2.2. Small-Angle Neutron Scattering. The microscopic structure of the networks was studied by performing small-angle neutron scattering (SANS) measurements in networks swollen to equilibrium. The measurements were done at the

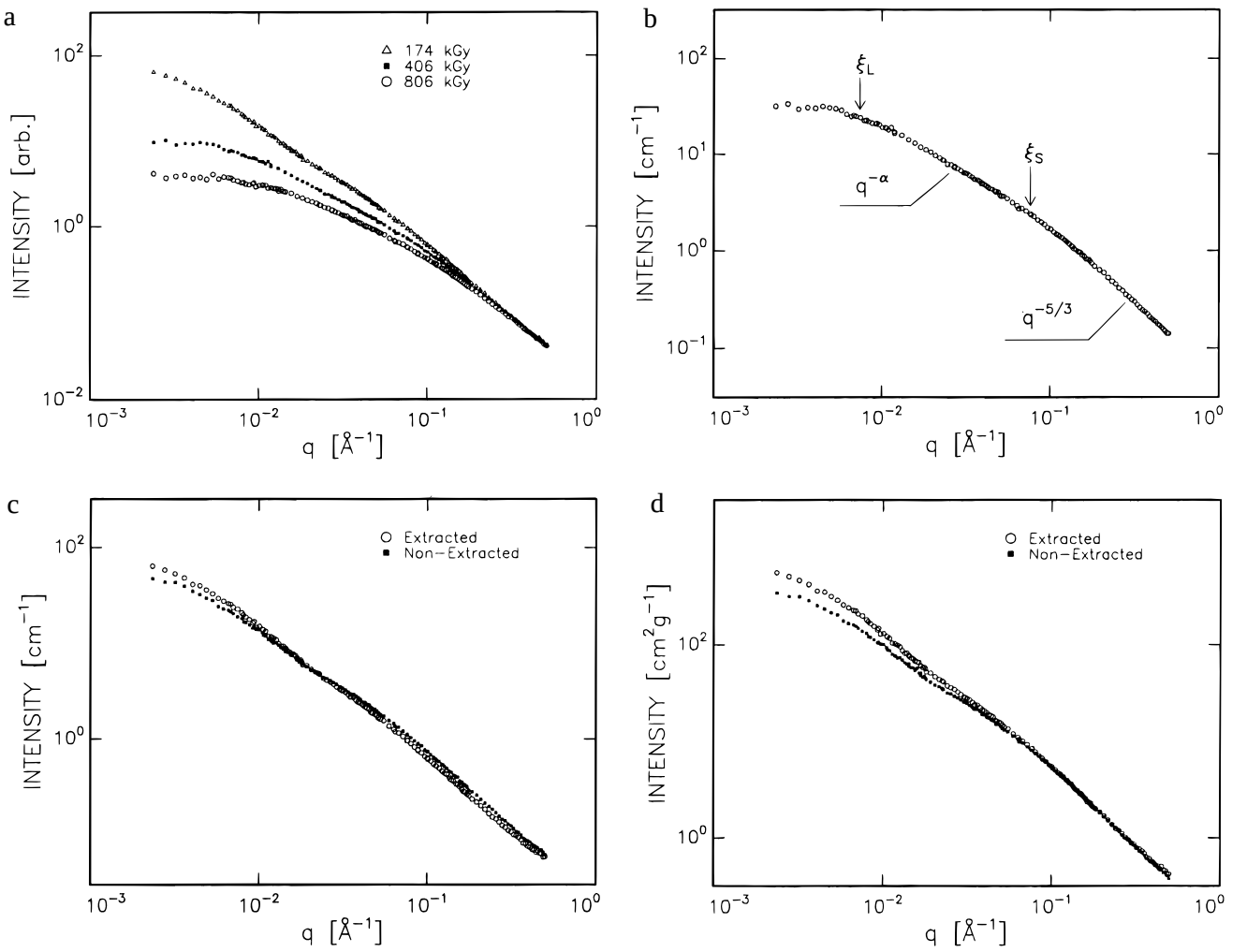

Figure 2. Small-angle neutron scattering from PDMS networks swollen to equilibrium in fully deuterated *p*-xylene. Double logarithmic plot of the scattering data as a function of scattering vector *q*. (a) Panel a shows three of the samples measured. The experimental spectra are arbitrarily scaled to the 116 kGy spectrum in order to better display the differences in scattering profile. The scaling factors used are closely proportional to the inverse polymer concentration present in each swollen gel. Panel b shows the spectrum obtained from the sample cross-linked to 406 kGy. The position of the two characteristic lengths and the two regions of linear behavior in the double logarithmic plot are pointed out (see text). Panel C shows a comparison between an extracted sample and the corresponding nonextracted one at equilibrium swelling (the irradiation dose was 174 kGy). Panel d shows the same spectra represented in c but scaled by polymer concentration.

SANS instrument installed at the DR3 reactor of the Risø National Laboratory. A fully deuterated solvent was used in order to obtain good contrast between polymer and solvent.

The extracted samples used were irradiated with six different doses: 116, 174, 200, 406, 806, and 999 kGy. Their gel weight fractions are, respectively, 0.66, 0.75, 0.79, 0.90, and 0.95. Two different samples both irradiated with 406 kGy but using different runs of the accelerator were measured. A nonextracted sample that was not included in the previous study was also measured. It was irradiated with 174 kGy.

In order to collect the scattered intensity over a broad scattering vector *q* range, each sample was measured using several different instrumental settings (neutron wavelength and sample-to-detector distance). The reciprocal space region explored in this way ranged from 0.003 to 0.45 Å^{-1} for all the samples measured.

The background coming from the quartz cuvette and deuterated solvent was subtracted from the raw scattering data. The contribution to the experimental background coming from other sources was measured by replacing the sample by a neutron absorber (B_4C), and it was also subtracted from the raw data. The data were normalized using the incoherent signal of a 1 mm thick water sample in order to correct for variations in detector efficiency and to have them on an absolute scale. Since the scattering patterns are azimuthally symmetrical, the data were reduced to the one-dimensional intensity, $I(q)$, that only depends on the absolute value of the scattering vector. The scattering spectra analysis was performed by a least-squares fitting program that includes the instrumental smearing effects using a resolution function,[12] and fits simultaneously the data recorded with the different spectrometer settings to the chosen model function. A parameter describing the incoherent background of the experiment was included in the fitting function.

3. Results and Discussion

3.1. Scattering Spectra. The scattering obtained from the extracted swollen networks shows clear similarities with the one obtained, previously, from the nonextracted swollen systems. Figure 2a shows a double logarithmic plot of the intensity scattered, $I(q)$, by extracted samples with different cross-link densities as a function of the scattering vector, *q*, and Figure 2b shows, also in a double logarithmic plot, the spectrum obtained from one of the samples cross-linked to 406 kGy. In order to make the differences in shape more evident, the spectra in Figure 2a are scaled in such a way that they overlap in the high *q* region. The scaling factors used are closely proportional to the inverse polymer concentration present in each swollen gel. As previously observed for the nonextracted samples,[11] it is possible to identify three distinct regions in each

spectrum. At high q, all the scattering curves have the same limiting behavior. The experimental points fall on a straight line with slope ~ -1.67, just like one would find in semidilute polymer solutions. At intermediate q, the scattering curves obey a $I \sim q^{\alpha}$ relationship but with an exponent α different from the limiting value at high q. Values of α between -1.3 and 1.65 were found. At low scattering vectors there is a cross-over to a region where the signal tends to become q independent. The transition between the different linear behaviors (in the double logarithmic plot) at high and intermediate q is clear for the samples cross-linked to the lower doses. With increasing irradiation dose, this cross-over becomes less and less pronounced. For the samples irradiated with doses higher than ~700 kGy it is hardly observable. On the other hand the low q cross-over to an almost q-independent signal becomes more and more evident with increasing dose, shifting to higher scattering vector values. Similar to the case of the nonextracted samples, for large values of the scattering vector, the spectra are very close to those obtained from polymer solutions with the same polymer concentration. On the contrary, at low q, the swollen network exhibits a clear excess scattering relative to the solution.

A comparison between spectra recorded from an extracted and the corresponding nonextracted network (Figure 2c) shows that, in the high q region, the intensity scattered by the nonextracted swollen system is systematically higher than the intensity scattered by the extracted one, whereas in the low q region the reverse is observed. It is also possible to see that the cross-over to a q-independent signal is present at a higher value of q in the nonextracted system. Divided by polymer concentration in the swollen systems (Figure 2d), the spectra are almost identical in the high q region, and the differences at low q are enhanced. Both the different position of the cross-over to a q-independent signal, and the lower value of the intensity scattered in the limit of zero scattering vector become clear.

3.2. The Model Expression. The scattering data were analyzed by means of the same model previously used in the analysis of the scattering data obtained from nonextracted samples. The similarities found between the scattering spectra obtained from swollen networks and from polymer solutions with the same polymer concentration in the high scattering vector region show that at small length scales, the monomers in the swollen network arrange in a self-avoiding walk just like in a semidilute solution. In addition, the value of q that marks the characteristic cross-over in the spectrum of the polymer semidilute solution is very close to the one at which the transition between the two power law behaviors of $I(q)$ occurs in the swollen gels. This suggests that, like for semidilute solutions, in the swollen gels there is a length scale below which single chain self-avoiding walk behavior is displayed. Furthermore the value of this characteristic length scale in the swollen network and in the corresponding solution must be very similar. This length is usually referred to as the *blob*[13] size. At larger length scales, the excess scattering relative to the corresponding semidilute solution reveals the presence of the large-scale heterogeneities of polymer concentration (i.e. larger than the equivalent solution blob size). These are assumed to result from the random cross-linking process: the solvent will be preferably absorbed in the regions where the local cross-link density is lower, because rearrangements of the network chains will be more difficult in regions where the density of cross-linking is locally higher.

The small and large-scale fluctuations present in these swollen gels were first modeled as being decoupled. For each one of them, the expressions used resembled Ornstein−Zernike functions (giving cross-overs to q-independent behavior below a certain characteristic q_{ξ} value, and having power law behaviors q^{β} for $q \gg q_{\xi}$). Both for the small- and large-scale terms the values of β found were always close to -1.67. The experimental data were, however, better fitted by using a structure factor typical of a fractal that includes explicitly the large- and small-scale characteristic cut-offs and better describes the cross-over regions. So, here, the large-scale density fluctuations are modeled as having a fractal structure corresponding to fluctuations in the density of *solution-like* blobs.

The scattered intensity is therefore approximated by

$$I(q) = \phi_N P(q) S(q) \tag{2}$$

$P(q)$ is the average form factor of one particle, which is here associated with blob of the solution with the same polymer concentration. ϕ_N is the number density of those particles, which are assumed to be assembled in a fractal arrangement. It must, however, be noted that the factorization in eq 2 is only strictly valid when the particles are centrosymmetric and monodisperse.

In order to obtain $P(q)$, the total scattering, $S_T(q)$, from a semidilute solution is used. In a semidilute solution all the chains are labeled, and $S_T(q)$ includes both intra- and inter-chains scattering. However, since the blobs are not correlated between themselves (by definition there is no correlation for distances larger than ξ_S), it is assumed that $S_T(q)$ is equal to the simple sum of the N_b form factor of all blobs. The expression used for $P(q)$ is

$$P(q) \simeq S_T/N_b \sim \xi^{5/3} \frac{(1 + q\xi_S)^{1/3}}{(1 + q^2\xi_S{}^2)} \tag{3}$$

This expression was found[11] to fit, within a front factor, the scattering from the polymer solutions over the q range accessed.

For the large-scale fractal structure, the correlation function between particles used was[14]

$$g_{large}(r) \sim r^{D_L} e^{-r/\xi_L} \tag{4}$$

where D_L is the fractal dimension and the exponential is a cutoff function introduced to account for the finite extent of the fractal correlations. The parameter ξ_L is the correlation length that represents the length scale at which the fractal density fluctuations approach the average density in the system. In reciprocal space, this gives[15]

$$S(q) = 1 + \frac{1}{(qr_0)^{D_L}} \frac{D_L \Gamma(D_L - 1)}{\left[1 + \frac{1}{(q\xi_L)^2}\right]^{(D_L-1)/2}} \times \sin[(D_L - 1)\arctan(q\xi_L)] \tag{5}$$

where Γ is the gamma function and r_0 is the characteristic dimension of the individual scatterer. In this expression the first term in the right hand side (=1) originates from the fact that at a sufficiently large scattering vector q the interference between particles

Table 1. Results Obtained form Small Angle Neutron Scattering Measurements in Networks Swollen to Equilibrium in Fully Deuterated *p*-Xylene[a]

dose (kGy)						
NE	E	ξ_S (Å)	ξ_L (Å)	$I(q \to 0)$ (cm^{-1})	A_1/A_2	excess [cm^{-1}]
	116	28.0	650.3	152.6	1.24	0.53
116		25.5	400.3	105.1	1.40	0.80
126		22.5	322.1	79.2	1.40	0.80
144		20.8	264.3	66.5	1.41	0.81
151		18.3	218.1	48.4	1.42	0.76
	174	20.0	361.1	78.6	1.21	0.48
174		17.3	220.1	46.9	1.42	0.71
	205	17.1	245.1	51.8	1.31	0.51
251		15.9	168.2	40.1	1.31	0.70
354		14.3	124.1	32.9	1.35	0.71
	406	11.8	120.3	34.7	1.36	0.66
	406	12.1	121.4	37.1	1.38	0.71
406		13.0	108.8	29.7	1.39	0.73
	806	9.2	70.1	16.3	1.24	0.43
806		10.0	64.3	14.3	1.29	0.57
1000		9.3	56.2	12.4	1.26	0.49

[a] ξ_S, particle size; ξ_L,, characteristic length for the large scale fluctuations; $I(q \to 0)$, intensity scattered in the limit of zero scattering vector; A_2/A_1, scaling factor between the particle and interference contributions to the overall scattering function; excess, excess contribution from the particle contribution.

is not observed and the scattering is dominated by the intraparticle scattering.

Since the particle is not well defined in the present context, the relative scaling between the self-correlation and interference contributions to the scattered intensity was left as a fitting parameter. The expression used to fit the experimental data was obtained by combining eqs 2, 3, and 5. It is

$$I(q) = I_p(q) + I_i(q) + C_{inc}$$

$$= A_1P(q) + A_2P(q)\frac{1}{q^{D_L}}\frac{D_L\Gamma(D_L-1)}{\left[1+\frac{1}{(q\xi_L)^2}\right]^{(D_L-1)/2}} \times \sin[(D_L-1)\arctan(q\xi)] + C_{inc} \quad (6)$$

where A_1 and A_2 are scaling factors for the self-correlation and interference contributions to the scattered intensity and C_{inc} is a constant that accounts for the incoherent background. The fitted values of C_{inc} reproduced the incoherent scattering expected from the hydrogen atoms present in the samples.

Due to the high number of parameters involved and following the results obtained for the nonextracted networks,[11] the value of the fractal dimension that characterizes the large-scale fluctuations has been first fixed to $D_L = 5/3$. The number of fitting parameters was initially further reduced by fixing ξ_S to the value of the corresponding semidilute solution. In this way only three parameters remain to be fitted. After determining the values of the other parameters, the release of the constraints imposed on D_L and ξ_S, does not introduce significant changes in their values.

Table 1 contains the results of fits to eq 6 for ξ_L, ξ_S, and the intensity scattered in the limit of zero scattering vector $I(q \to 0)$. The table also includes values for the ratio A_1/A_2 (to be compared with the value unity in eq 5), and the excess particle contribution to the intensity scattered in the limit of zero scattering vector, defined as

$$\text{excess} = (A_1 - A_2)P(q \to 0) \quad (7)$$

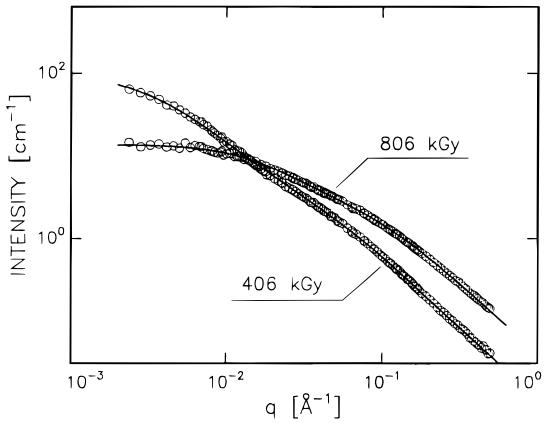

Figure 3. Experimental scattering spectra and fitted function (solid line) as a function of scattering vector q in a double logarithmic plot for two different networks swollen to equilibrium in fully deuterated *p*-xylene. The irradiation doses were (a) 116 and (b) 806 kGy. The symbol size is of the order of the larger error bar.

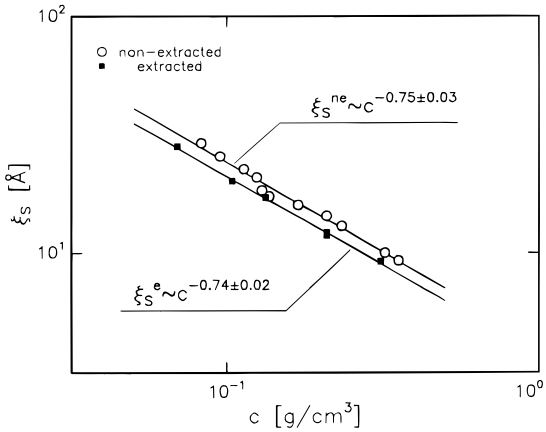

Figure 4. Double logarithmic plot representing the characteristic length ξ_S (average particle size) as a function of polymer concentration in the swollen systems. Open circles indicate nonextracted systems, and filled squares, extracted networks. The solid lines are the results of fits to the experimental points. The symbol size is of the order of the larger error bar.

The quality of the fits is excellent for all the samples measured ($\chi^2 \leq 1.5$). Figure 3 shows the fit functions to spectra obtained from two networks of very different cross-link densities.

3.3. Scaling Relations for Extracted and Nonextracted Swollen Gels. Figure 4 shows the values, obtained for ξ_S for both extracted and nonextracted networks, plotted as a function of polymer concentration, c_p, in the swollen systems in a double logarithmic plot.

For the correlation length ξ_S, of the small-scale concentration fluctuations, a linear fit to the points gives a slope -0.74 ± 0.02, so $\xi_S \sim c_p^{-3/4}$ for the swollen networks, both extracted and nonextracted, as for pure semidilute solutions.

Comparing ξ_S between extracted and nonextracted networks with the *same equilibrium swelling ratio* ($Q = V_{eq}/V_{dry}$), shows that ξ_S is larger for the extracted network. The reason must be that the extracted and the parent nonextracted network (same irradiation dose) have close swelling ratios Q, but different polymer concentrations c_p. The polymer concentration in the swollen systems obeys eq 1. This means that, at equilibrium swelling, more free space is available for

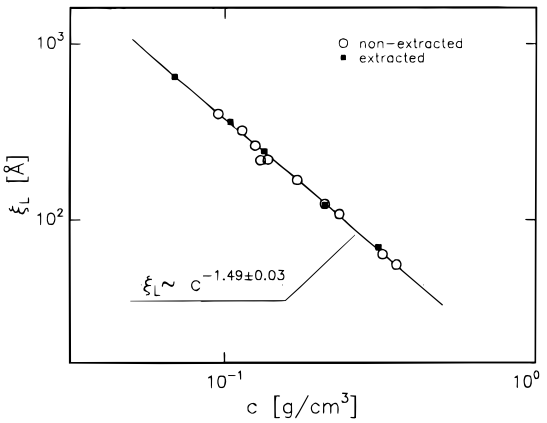

Figure 5. Double logarithmic plot representing the correlation length for the large-scale fluctuations ξ_L as a function of polymer concentration in the swollen systems. Open circles indicate nonextracted systems, and filled squares, extracted networks. The solid line is the results of a fit to the experimental points obtained from the extracted swollen networks. The symbol size is of the order of the larger error bar.

the chains to rearrange, particularly those that are loosely attached to the network.

On the other hand, comparing ξ_S between extracted and nonextracted networks *at the same polymer concentration*, c_p, shows that ξ_S is slightly lower for the extracted network. This may be explained by the fact that comparing results at the same polymer concentration in the swollen systems corresponds, here, to comparing results for networks with different cross-link densities: in order to have the same polymer concentration at equilibrium swelling, the extracted network will have to be irradiated at a higher dose. This explanation is related to the possibility of the existence of some polydispersity in the distribution of blob sizes: if the local polymer concentration is varying in the network, the size of the blob may vary as well.

The observed ξ_S for both extracted and nonextracted networks are slightly higher than those of the seimdilute solution with the same polymer concentration: this could result from the averaging process over a polydisperse ensemble of blobs (the weight favors the larger blobs). The small differences observed suggest, however, that the effect is not too important. But note that this would have another consequence, namely, $\xi_S^{ne} > \xi_S^{e}$ at same c_p. In fact, in the nonextracted networks, the soluble components are expected to occupy preferably the regions of weaker cross-linking, where the polymer concentration is lower (the larger holes available when the network is swollen). Then, in the ensemble of all chains (linked and not linked), the proportion of larger blobs will be higher when compared to the case in which all the chains are linked (the extracted network). These arguments would explain the fact that, at the same polymer concentration, ξ_S is slightly larger for the nonextracted network than for the extracted one.

The results for the second correlation length, ξ_L, characteristic of the large-scale heterogeneities will now be discussed. ξ_L^{e} (extracted networks) and ξ_L^{ne} (nonextracted networks) are plotted in Figure 5 as a function of polymer concentration in the swollen systems. The values of $\log(\xi_L^{e})$ are approximately linearly dependent on $\log(c_p)$. A linear fit to the experimental points give the slope -1.49 ± 0.03 (a value close to $-3/2$), implying the scaling relation:

$$\xi_L^{e} \sim c_p^{-1.49} \tag{8}$$

At the same swelling ratio, Q, the observed correlation length ξ_L is larger for an extracted network than for the corresponding nonextracted one (see Table 1). However, plotted as a function of c_p, the values of ξ_L for the extracted networks fall, within experimental accuracy, on the *same straight line* that fits the experimental points obtained from the nonextracted networks.

Let us consider again the localization of the soluble components in the nonextracted networks. We propose that it depends on their molecular weight. The low molecular weight ones can be more uniformly distributed, because of their higher entropy of mixing. Due to this uniformity and also to their small size, their contribution to the low q scattering will be a flat one, looking like a constant background, with no effect on ξ_L^{ne}. The large molecular weight components may, on the contrary, have structures similar to those of clusters of the same size belonging to the connected structure. About their spatial distributions two opposite possibilities can occur:

(i) They are distributed in an homogeneous way. In this case, they will not modify the spatial distributions of the connected structure, and, at the same concentration of polymer linked to the network

$$\xi_L^{ne} \simeq \xi_L^{e} \qquad c_p^{linked} = \text{constant} \tag{9}$$

and at the same total concentration

$$\xi_L^{ne} > \xi_L^{e} \qquad c_p^{total} = \text{constant} \tag{10}$$

because, in the nonextracted network, the soluble components, which are "neutral", allow space available for the heterogeneities of the connected structure to unfold.

(ii) Alternatively, the large molecular weight components may be distributed nonuniformly. In an extreme case, because their structure is similar to the one of the clusters of the same size present in the network, they may have a similar spatial distribution, i.e., be undistinguishable. Then,

$$\xi_L^{ne} \simeq \xi_L^{e} \qquad c_p^{total} = \text{constant} \tag{11}$$

and,

$$\xi_L^{ne} < \xi_L^{e} \qquad c_p^{linked} = \text{constant} \tag{12}$$

because in the latter case (eq 12) the nonextracted network has a higher total polymer concentration.

The observed result agrees with eqs 11 and 12, thus supporting the idea that the large molecule soluble clusters behave as the connected clusters of the same size present in the network. This agrees with the picture of a unique self-semilarity of clusters over a broad range of irradiation, below and above the gel point.

Figure 6 displays a double logarithmic plot of the intensity scattered in the limit of zero scattering vector, $I(q \to 0)$, versus polymer volume fraction in the swollen systems. A linear fit to the experimental points gives a slope -1.47 ± 0.07, a value that like the one obtained from nonextracted swollen gels[11] is close to $-3/2$, and implies the scaling relation

$$I(q \to 0) \sim c_p^{-1.47} \tag{13}$$

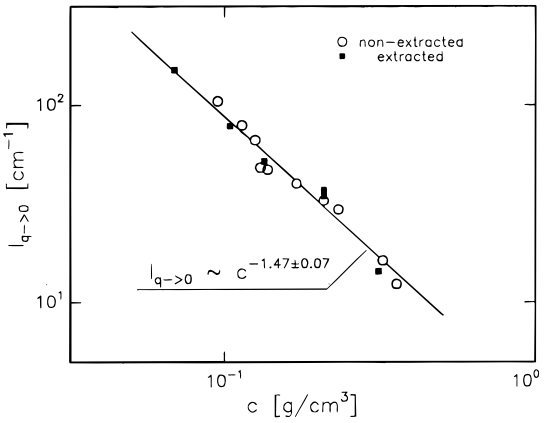

Figure 6. Double logarithmic plot of the intensity scattered in the limit of zero scattering vector as a function of polymer concentration in the swollen systems. Open circles indicate nonextracted systems, and filled squares, extracted networks. The solid line is the results of a fit to the experimental points obtained from the extracted swollen networks. The symbol size is of the order of the larger error bar.

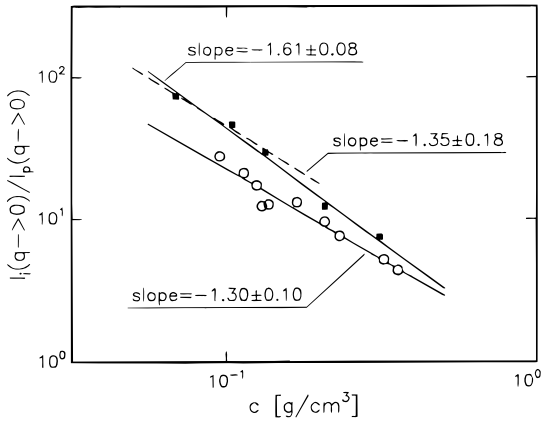

Figure 7. Double logarithmic plot of the scale between the interference and particle contributions to the intensity scattered in the limit of zero scattering vector as a function of polymer concentration in the swollen systems. Open circles indicate nonextracted systems, and filled squares, extracted networks. The solid lines are the results of a fit to the experimental points obtained from the extracted swollen networks. The broken line is a fit to the values obtained for the three extracted networks with lower polymer concentration. The symbol size is of the order of the larger error bar.

As expected from the enhancement of ξ_L upon extraction, $I(q \to 0)$ is larger, at constant Q, for an extracted network than for the corresponding extracted one. Similarly, as observed for ξ_L, the intensities $I^e(q \to 0)$ and $I^{ne}(q \to 0)$ fall on the same line, within experimental accuracy, when plotted versus c_p. This also points to the conclusion that, in the swollen systems, the extractable components conform essentially as the network strands do. Similar behavior has been reported from swelling pressure measurements performed on chemically cross-linked poly(vinyl acetate) (PVAc) gels swollen in toluene and containing free PVAc chains.[16]

The ratio between the interference, $I_i(q \to 0)$, and self-correlation, $I_p(q \to 0)$, contributions to the intensity scattered in the limit of zero scattering vector for both extracted and nonextracted networks are presented in Figure 7 as a function of polymer volume fraction in the swollen gels. This ratio also scales with the polymer volume fraction. There is however a clear difference between the exponents for the extracted and nonextracted networks. A linear fit to the experimental points obtained from the nonextracted samples gives a slope -1.30 ± 0.1, whereas for the extracted ones the slope is -1.61 ± 0.07. The simplified picture that strictly validates the use of eq 2, in which the *blobs* are considered as true particles with no polydispersity, leads to a scaling relation:[11]

$$\frac{I_i(q \to 0)}{I_p(q \to 0)} \sim \left(\frac{\xi_L}{\xi_S}\right)^{5/3} \sim c_p^{-5/4} \qquad (14)$$

between the self-correlation and interference contributions to the intensity scattered at zero scattering vector. The results from the nonextracted networks agree within the error bar with the expected $-5/4$, whereas for the extracted networks, the exponent is clearly higher. The deviations observed are the result of an excess *particle* contribution to the overall scattered intensity and/or from the nature of the *particles* involved. This excess contribution is reflected in the values of the ratio between the fitting parameters A_1 and A_2. It is always larger than unity (see Table 1). In the extracted networks the excess scattering could be attributed to the presence of structures that are weakly

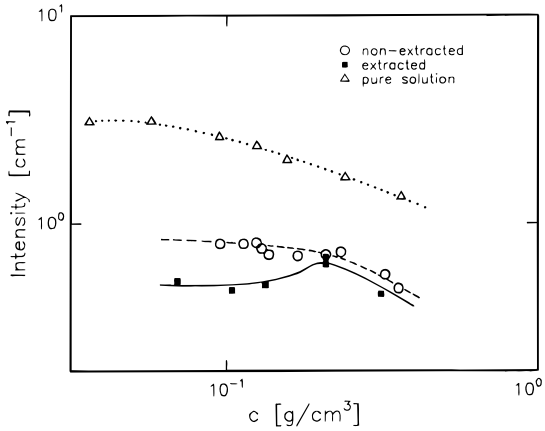

Figure 8. Double logarithmic plot of the excess particle contribution to the intensity scattered in the limit of zero scattering vector as a function of polymer concentration in the swollen systems. Open circles indicate nonextracted systems; filled squares, extracted networks; and open triangles, pure polymer solutions. The lines are guides to the eye. The symbol size is of the order of the larger error bar.

connected to the network and that are free to spread out through the larger spaces available in such a way that the interaction with the surrounding network strands becomes weak. In the case of the nonextracted systems, an additional contribution resulting from the lower molecular weight material present in the extractable components must be considered.

The excess *particle* scattering i.e., $(A_1 - A_2)\,P(q \to 0)$ is shown in a double logarithmic plot as a function of polymer concentration in Figure 8. In the same plot the intensity scattered in the limit $q \to 0$ from pure solutions (obtained previously[11]) is displayed for comparison. For both the extracted and nonextracted systems the excess contribution is considerably lower than the intensity scattered by the pure solution. This means that the fraction of soluble components responsible for this excess is considerably lower than unity both in the extracted and nonextracted networks. The values are somewhat scattered, but nevertheless, it is possible to observe a difference in behavior between the extracted and nonextracted systems. For the nonex-

tracted samples the excess contribution is roughly constant at the lower polymer concentrations, and decreases with increasing c_p, the general trend being, however, to essentially reproduce the curve obtained from the pure solution (dotted line in the plot). For the extracted samples different behaviors were observed depending on the level of irradiation dose. For the samples that were irradiated to higher doses the excess contribution is very close to the one obtained from the nonextracted networks. For those that were irradiated to lower doses the contribution is smaller than for the nonextracted samples. The cross-over between the two cases occurs at a concentration that corresponds to the equilibrium swelling concentration of a network irradiated to ~150 kGy. The differences observed cannot be completely accounted for by a complete removal of the soluble components in the extracted network. In particular the more pronounced decrease at low polymer concentration (corresponding to irradiation doses below ~150 kGy) must be related to the efficiency of the washing process. It must be noted that for these networks it was found[11] that the irradiation dose at which each polymer chain in the network has, on the average, two cross-links is ~120 kGy. For lower irradiation doses the open spaces in the network will then be large and so it will be easy for the extractable components to diffuse out of the swollen system. For larger irradiation doses, the amount of nonnetwork material that will be trapped in the network is expected to increase with increasing dose. This effect (eq 10) can qualitatively account for the deviations from the predicted $-5/4$ power law. In this respect, a fit through the three lower concentration points, for which the trapping effect is not expected to be important, gives back a slope -1.35 ± 0.18 in agreement with the value for nonextracted gels, and eq 14.

3.4. Comparison to Models. First, results expected from theories based on the percolation model for the swelling of gels will be recalled. For cross-linking densities below the critical percolation density (corresponding to irradiation doses $r = r_g - \epsilon$, where r_g is the gelling dose and ϵ is a positive value verifying $\epsilon \ll r_g$), the gel point is not reached. The system is an ensemble of clusters not connected at macroscopic scale. However, the theory developed to describe the swelling of gels prepared at $r = r_g - \epsilon$ by cross-linking small polyfunctional units[17] is an important reference of the theories that describe the swelling of networks, and will therefore be briefly recalled. Percolation clusters made out of small polyfunctional units have a molecular weight distribution, $P(N) \sim N^{-\tau} \exp(N/N^*)$, where τ is the exponent that characterizes the mass distribution ($\tau = 2.2$), and N^* is the maximum molecular weight of the distribution (close to the Z-average, N_Z) that diverges when $r \rightarrow r_g$. In the reaction bath each cluster has a fractal structure characterized by a fractal dimension $D_p = 2.5$. By the addition of solvent the clusters swell, and in the dilute regime, each cluster has a fractal dimension $D_s = 2.0$. In the reaction bath the clusters are completely interpenetrated, the small ones filling the holes present in the larger ones. The dilution process consists in progressively disinterpenetrate the clusters: in the early stages the small clusters are removed, and the swelling process continues by removing clusters of increasingly larger mass. As long as all the clusters are not completely swollen, the concentration regime is called semidilute, and the corresponding solutions are characterized by a correlation length ξ_L, that is associated with the length under which the clusters are in a swollen conformation. The complete disinterpenetration is achieved at a certain concentration c^*, related to the largest cluster mass. The scattering function predicted for these systems is, for $c < c^*$ and $q > 1/\xi_L$, a power law of q with an exponent $-D_F(3 - \tau) = -1.6$. The term $(3 = \tau)$ is a consequence of the high polydispersity that characterizes the mass distribution.[18] This power law is expected to cross-over, at $q \sim 1/\xi_L$, to a weak q dependence. The scattered intensity is predicted to obey the following limiting behavior: $I(q \rightarrow 0) \sim c^{5/3}$.

On the other side of the percolation threshold, i.e., for $r = r_c + \epsilon$, the situation can be treated in a similar way. The main difference is the existence of an infinite cluster. In this case the equilibrium concentration is identified with the overlap concentration of the clusters of different sizes. At equilibrium swelling, the swollen network is assumed to have a structure similar to the one of a semidilute solution of percolation clusters. Thus the power laws predicted for the semidilute case, mentioned above, are also expected to hold when $r = r_c + \epsilon$.

When the units that make up the clusters are chains, instead of small polyfunctional units, the model is still applied after rescaling to the size of the chain.[19] For lengths smaller than the characteristic size of a chain, a behavior similar to the one of linear chains in solution is expected. Reference 18 treats both types of building units: small units and chains, and in particular it addresses the "vulcanization case" (when each chain can be attached by more than one cross-link), a situation similar to the one explored in this paper.

The percolation model has also been used in a slightly different case, in which the gel is produced from a semidilute solution of very long chains, each one made out of blobs of size ξ_S.[20] Producing the cross-linking in solution creates clusters of blobs, and these will percolate through the system at a certain cross-linking density (~1 cross-link per blob), that will be considerably higher than the critical density defining the gel point for the system of chains (~1 cross-link per chain). Under additional solvent absorption, the clusters of attached blobs are expected to swell less than the free blobs. This will give rise to large concentration fluctuations, which are modeled by the dilution of percolation clusters. The laws predicted for the concentration dependence of the correlation length and the intensity in the limit of zero scattering vector are the same as those predicted by the model of dilution of percolation clusters referred above.

The samples used in this work were irradiated to doses considerably higher than the "gelling" dose, but it is possible that some properties of networks in the vicinity of the gelling dose are relevant here. Note that the structure of the cross-linked networks is influenced by the initial polydispersity of the molecular weight distribution of the precursor polymer melt and that in particular the gel point for the system is essentially determined by the molecular weight of the larger chains present in the melt. So, many clusters formed by the linking of smaller chains will be either loosely attached to the network or not attached at all, even for irradiation doses considerably higher than the gelling dose.

The power laws observed experimentally are relatively close to those predicted by percolation models, and it is worth remarking that power laws with similar exponents have also been observed in statistical gels

produced by multiple cross-linking of long linear chains in solution,[21] in spite of the differences in the conditions of cross-linking. Here $I(q \to 0) \sim c_p^{-1.5}$ compares with $c_p^{-1.6}$, $\xi_L \sim c_p^{-1.5}$ compares with $c_p^{-1.67}$, and $S(q) \sim c_p^{-1.67}$ compares with $c_p^{-1.6}$ for $1/\xi_L < q < 1/\xi_S$. Also the observed large q behavior, ($q > 1/\xi_S$), is in agreement with the predictions of the percolation model when the building units of the clusters are chains.

Concerning the power law behavior of $S(q)$ at intermediate q, it must be noted that the value -1.6, expected from the percolation model, results from the polydispersity typical of the mass distribution of percolation clusters, each of them characterized by a fractal dimension of 2. When the system is washed, the smaller components of the mass distribution are removed, so extraction is equivalent to the introduction of a low cutoff, N_w in the mass distribution. This would lead to two different power laws for the behavior of $S(q)$ at intermediate q. The typical size, ξ_u, of the cluster of mass N_w would mark a cross-over between a region, ($1/\xi_L < q < 1/\xi_w$), where the exponent -1.6 is observed, to another region, ($1/\xi_w < q < 1/\xi_S$), where the power law would have a limiting value ~ -2. In the experimental data there is no evidence of any kind of enhancement of the value of the slope upon extraction. It could however be argued that the cutoff is not sharp enough for the effect to be observed.

It is however noticeable that, although the general features predicted by the percolation models have been observed, namely the power law behaviors, the exponents found here are slightly but systematically different from the percolation ones. The difference is not very large and the model cross section used could be partially responsible for them, although the results obtained are completely consistent with the expression used. On the other hand the deviations from the power laws expected from percolation models could be ascribed to the particularities of the molecular weight distribution that characterizes the polymer melt used (especially the large amount of low molecular weight material present). In connection to this a different model[11] has been proposed. It starts from the remark that the irradiated system has a connected path that carries the stresses for the system, and is essentially formed by the larger masses present in the precursor polymer. Attached to the connected path by only one or two cross-links, there will be single polymer chains and small branched structures that result from the random cross-linking process. Upon solvent absorption, each strand of the connected structure will appear "hairy", due to the dangling ends. At large scale such a strand behaves like a linear part of a chain, for which excluded volume effects would appear like those observed for linear chains in solution. The excluded volume free energy would be proportional as usual to the square of the local concentration in monomers, which here includes all the dangling ends and therefore is large. Such a rescaled linear behavior would stop at distances ξ_L of the order of the one between two junctions of the connected structure, above which the latter is a regular net. Such a model is quite different from a percolation picture. On the other hand, at small length scales, most of the pendent chains can, themselves, freely rearrange and this will lead to a behavior typcial of single chains in solution with the establishment of excluded volume around each arm, i.e., locally the chains will also be swollen.

In the previous work on nonextracted swollen gels[11] it was found that the large-scale concentration fluctuations were correlated up to distances that scale with the average number of monomers in between elastically effective cross-links, N_C, as $N_C \sim \xi_L^{5/3}$ giving experimental support of the excluded volume picture.

By picturing the system at large length scales as a kind of a self-avoiding walk of units with average size ξ_S, the following scaling relations are expected: $\xi_L \sim c_p^{-3/2}$, $\xi_S \sim c_p^{-3/4}$, $\xi_L/\xi_S \sim c_p^{-3/4}$, $I(q \to 0) \sim c_p^{-3/2}$. These exponents are in very good agreement with those obtained from experiment.

In this model, the presence of structures not incorporated in the macroscopic network is not expected to change qualitatively the profile of the scattering patterns. This applies whether the soluble components are removed from the irradiated systems during the washing process, or not. The only requirement is that they have structurs similar to those present in regions of the macroscopic cluster. This was also observed in the experiment. The presence of the extractable components is simply to change the overall concentration of polymer in the equilibrium swollen systems, and a swollen system that includes extractable material is, within experimental accuracy, equivalent to a washed swollen network that had been irradiated to a higher dose.

The data were not compared to other models quoted previously.[6,7] These models imply minimization of the free energy using linear elasticity theories, and assume that the networks are homogeneous,[7] or that they have uncorrelated heterogeneities.[6] The net-works studied here must be far from this description. These models have been recently compared[22,23] wtih experimental data that displayed behaviors close to the ones reported here,[10,21] and clear discrepancies were observed. We believe that similar differences would be found with our data as well.

4. Summary and Conclusions

As for nonextracted swollen samples, the results obtained from swollen extracted networks, show the presence of large-scale concentration fluctuations of polymer concentration, and single chain behavior at small length scales. A model cross-section typical of a fractal arrangement of particles, previously used in the analysis of the scattering data obtained from nonextracted swollen networks, fits well the data from extracted samples. The fractal dimension of $^5/_3$ was found to characterize the fluctuations for all the networks studied, and these had been prepared to very different cross-link densities. The results confirm a series of power laws found previously for nonextracted networks relating the correlation lengths ξ_L and ξ_S, and the intensity scattered in the limit of zero scattering vector to the polymer volume fraction: $\xi_L \sim c_p^{-3/2}$, $\xi_S \sim c_p^{-3/4}$, $\xi_L/\xi_S \sim c_p^{-3/4}$, $I(q \to 0) \sim c_p^{-3/2}$. As in the case of the nonextracted samples the qualitative features of the scattering spectra, and the exponents found are close to predictions of models based on percolation theory. There are, however, some differences in the exponents found. These differences could be partially ascribed to the model cross section used because, it only gives a consistent picture for a monodisperse system of particles. The deviations could also result from the particularities of the mass distribution in the polymer melt used—a very polydisperse distribution with particularly a large amount of very small molecular weight material.

A different model suggested by the characteristics of the mass distribution of the precursor melt, was also used. It explains the volume swelling as resulting from the separation of the chains at all length scales. At large scale, the structure of the swollen network is described by the establishment of some kind of excluded volume interaction between large connected linear-like units, each including several polymers, which themselves swell when the network goes from the dry state to the maximum equilibrium swelling.

Furthermore, the experimental points obtained from the extracted and nonextracted systems for ξ_L and $I(q \rightarrow 0)$ fall, within experimental accuracy, on the same line. There is, thus, the clear suggestion that, in the nonextracted swollen system, the larger masses present in the extractable components act essentially as network strands.

Finally, it is interesting to note that, for these networks that were prepared by irradiation to intermediate doses, the discussion of structural parameters in terms of cross-linking density can be transformed into a completely equivalent discussion in terms of polymer concentration, and this is independent of the irradiated systems being washed or not.

Acknowledgment. A.F. acknowledges the financial support of an C.E.C. research bursary (contract BREU CL900378). We are grateful to Walter Batsberg for discussions concerning sample preparation and sample extraction, and to Lotte Hansen for performing most of the extraction work. We also thank Arne Miller and the staff of the Risø National Laboratory's 10 MeV Electron Accelerator for performing the irradiation of the samples.

References and Notes

(1) Flory, P. J. *Principles of Polymer Chemistry*; Cornell University Press: Ithaca, NY, 1953.

(2) James, H.; Guth, E. *J. Polym. Sci.* **1949**, *4*, 153.

(3) Bastide, J.; Leibler, L. *Macromolecules* **1989**, *21*, 2647.

(4) Higgs, P.; Ball, R. *J. Phys.* **1988**, *49*, 1785.

(5) Geissler, E.; Horkay, F.; Hecht, A. M. *Phys. Rev. Lett.* **1993**, *4*, 645.

(6) Onuki, *J. Phys. II* **1992**, *2*, 45.

(7) Rabin; Bruinsma. *Europhys. Lett.* **1992**, *20*, 79.

(8) Boué, F.; Bastide, J.; Buzier, M.; Collete, C.; Lapp, A.; Herz, J. *Prog. Colloid Polym. Sci.* **1987**, *75*, 152.

(9) Boué, F.; Bastide, J.; Buzier, M.; Lapp, A.; Herz, J.; Vigils, T. *Colloid Polym. Sci.* **1991**, 195.

(10) Zielinsky, F. H. Thesis, University Pierre et Marie Curie (Paris VI), Paris, France, 1991. Zielinksy, F. H.; Buzier, M.; Lartigue, C.; Bastide, J., Boué, F. *Prog. Colloid Polym. Sci.* **1992**, *90*, 115.

(11) Falcão, A. N.; Pedersen, J. S.; Mortensen, K. *Macromolecules* **1993**, *26*, 5350.

(12) Pedersen, J. S.; Posselt, D.; Mortensen, K. *J. Appl. Crystallogr.* **1990**, *23*, 321.

(13) de Gennes, P. *Scaling Concepts in Polymer Physics*; Cornell University Press: Ithaca, NY, 1979.

(14) Freltolt, T.; Kjems, J. K.; Sinha, S. K. *Phys. Rev. B* **1986**, *33*, 269.

(15) Teixeira, J. *J. Appl. Crystallogr.* **1988**, *21*, 781.

(16) Hecht, A. M.; Stanley, H. B.; Geissler, E.; Horkay, F.; Zrinyi, M. *Polymer* **1993**, *34*, 2894.

(17) Daoud, M.; Leibler, L. *Macromolecules* **1988**, *21*, 1497.

(18) Martin, J. E. *J. Appl. Crystallogr.* **1986**, *19*, 25.

(19) Johner, A.; Daoud, M. *J. Phys.* **1989**, *50*, 2147.

(20) Bastide, J.; Leibler, L. *Macromolecules* **1988**, *21*, 2647.

(21) Mendes, E. Thesis, University Louis Pasteur, Strasbourg, France, 1991. Mendes, E.; Lindner, P.; Buzier, M.; Boué, F.; Bastide, J. *Phys. Rev. Lett.* **1991**, *66*, 1595.

(22) Ramzi, A.; Zielinski, F. H.; Bastide, J.; Boué, F. To be submitted for publication.

(23) Mendes, E.; Boué, F.; Bastide, J. To be submitted for publication.

MA941014Q